Cytogenetic and Genome Research

Original Article

Cytogenet Genome Res 2020;160:255–263
DOI: 10.1159/000508012

Received: January 7, 2020
Accepted: April 7, 2020
Published online: June 16, 2020

# Truncated RUNX1 Generated by the Fusion of *RUNX1* to Antisense *GRIK2* via a Cryptic Chromosome Translocation Enhances Sensitivity to Granulocyte Colony-Stimulating Factor

Akihiro Abe[a] Yukiya Yamamoto[a] Akira Katsumi[b] Hideyuki Yamamoto[a] Akinao Okamoto[a] Yoko Inaguma[a] Chisako Iriyama[a] Masutaka Tokuda[a] Masataka Okamoto[a] Nobuhiko Emi[a, c] Akihiro Tomita[a]

[a]Department of Hematology, Fujita Health University, Toyoake, Japan; [b]Department of Hematology, National Center for Geriatrics and Gerontology, Obu, Japan; [c]Department of Hematology, National Hospital Organization Toyohashi Medical Center, Toyohashi, Japan

**Keywords**
Acute myeloid leukemia · *GRIK2* · Missplicing · *RUNX1* · Translocations

**Abstract**
Fusions of the Runt-related transcription factor 1 (*RUNX1*) with different partner genes have been associated with various hematological disorders. Interestingly, the C-terminally truncated form of RUNX1 and *RUNX1* fusion proteins are similarly considered important contributors to leukemogenesis. Here, we describe a 59-year-old male patient who was initially diagnosed with acute myeloid leukemia, inv(16)(p13;q22)/*CBFB-MYH11* (FAB classification M4Eo). He achieved complete remission and negative *CBFB-MYH11* status with daunorubicin/cytarabine combination chemotherapy but relapsed 3 years later. Cytogenetic analysis of relapsed leukemia cells revealed *CBFB-MYH11* negativity and complex chromosomal abnormalities without inv(16)(p13;q22). RNA-seq identified the glutamate receptor, ionotropic, kinase 2 (*GRIK2*) gene on 6q16 as a novel fusion partner for *RUNX1* in this case. Specifically, the fusion of *RUNX1* to the *GRIK2* antisense strand (*RUNX1-GRIK2as*) generated multiple missplicing transcripts. Because extremely low levels of wild-type *GRIK2* were detected in leukemia cells, *RUNX1-GRIK2as* was thought to drive the pathogenesis associated with the *RUNX1-GRIK2* fusion. The truncated RUNX1 generated from *RUNX1-GRIK2as* induced the expression of the granulocyte colony-stimulating factor (G-CSF) receptor on 32D myeloid leukemia cells and enhanced proliferation in response to G-CSF. In summary, the *RUNX1-GRIK2as* fusion emphasizes the importance of aberrantly truncated RUNX1 in leukemogenesis.


The Runt-related transcription factor 1 (RUNX1), also known as acute myeloid leukemia 1 protein (AML1) or core-binding factor subunit alpha-2 (CBFA2), plays a crucial role in hematopoiesis. Consequently, genetic alterations in *RUNX1* can induce various hematological diseases [Owen et al., 2008; Ichikawa et al., 2013]. The fusion of *RUNX1-RUNX1T1*, located at t(8;21)(q22;q22), is the most frequently detected fusion gene in acute myeloid leukemia (AML) and is associated with disease maturation [Miyoshi et al., 1993]. *RUNX1* also fuses with many other partner genes in hematological malignancies [De Braekeleer et al., 2009]. In most such fusions, *RUNX1* re-

karger@karger.com
www.karger.com/cgr

Karger

Akihiro Abe
Department of Hematology, Fujita Health University
98 Dengakugakubo, Toyoake
Aichi, 470-1192 (Japan)
aakihiro@fujita-hu.ac.jp

tains the runt homology domain (RHD) but loses the C-terminal transcription activation domain (TAD), suggesting that RUNX1 dysfunction is a common feature in leukemogenesis. This aberrant, C-terminally truncated form of RUNX1 is considered important in out-of-frame fusions and fusions to the antisense strands of partner genes [Maki et al., 2012; Cancer Genome Atlas Research Network, 2013; Giguère and Hébert, 2013]. For example, a short RUNX1a isoform that retains the RHD but lacks the TAD promoted the engraftment of hematopoietic stem cells in an irradiated mouse model and expansion of immature hematopoietic cells [Tsuzuki et al., 2007]. Similar to RUNX1 fusion proteins, the expression of a truncated RUNX1 protein in immature hematopoietic progenitors is considered as an important factor in the development of leukemia [Rodriguez-Perales et al., 2016].

Here, we present a case of therapy-related AML in a patient who harbored a novel variant *RUNX1* fusion gene resulting from a cryptic rearrangement between 6q16 and 21q22. This fusion yielded a truncated form of RUNX1 that enhanced the sensitivity of leukemia cells to granulocyte colony-stimulating factor (G-CSF).

## Materials and Methods

*RT-PCR Analysis*

TRIzol (Invitrogen, San Diego, CA, USA) was used to isolate total RNA from mononuclear bone marrow cells of our patient. Next, cDNA was synthesized from total RNA using the PrimeScript 1st strand cDNA Synthesis Kit (Takara, Otsu, Japan). RT-PCR amplification was then performed using the Platinum *Taq* DNA Polymerase High-Fidelity PCR kit (Invitrogen), oligonucleotide primers, and a 35-cycle protocol. The primers used for the PCR analysis are listed in online supplementary Table 1 (see www.karger.com/doi/10.1159/000508012 for all online suppl. material). The PCR reaction products were electrophoresed on 2% agarose gels and stained with ethidium bromide.

*Next-Generation Sequencing*

Total RNA was extracted from the patient's frozen relapse-phase bone marrow cells using the RNeasy Mini-kit and QIAshredder spin column (both Qiagen, Hilden, Germany) according to the manufacturer's instructions. The integrity and purity of the total RNA were assessed using an Agilent Bioanalyzer (Agilent Technologies, Santa Clara, CA, USA). Subsequently, cDNA was generated using the NEBNext Ultra RNA Library Prep Kit for Illumina (New England Biolabs, Ipswich, MA, USA), fragmented, and processed for Illumina library preparation using NEBNext reagents (New England Biolabs). The libraries were subsequently submitted for Illumina HiSeq1500 sequencing (Illumina, San Diego, CA, USA) according to standard protocols. Approximately 51 million paired-end 100-nucleotide reads were analyzed and aligned against the human hg19 reference genome using CLC genome workbench v8.0 (Qiagen, Aarhus, Denmark). The fusion genes were also analyzed using TopHat-Fusion [Kim and Salzberg, 2011] and deFuse [McPherson et al., 2011] software.

*Cell Culture*

The interleukin-3 (IL-3)-dependent murine myeloid cell line, 32D, was maintained in Iscove's modified Dulbecco's medium (IMDM; Sigma, St. Louis, MO, USA) supplemented with 10% FBS (Gibco, Grand Island, NY, USA) and 1 ng/mL murine IL-3 (mIL-3; Kirin, Tokyo, Japan). G-CSF was purchased from R&D systems (Minneapolis, MN, USA).

*DNA Constructs and Retroviral Vector*

*RUNX1-GRIK2as* cDNA of variant d (Fig. 2B) was cloned from RNA isolated from the patient's leukemia cells via RT-PCR. The amplified DNA construct was inserted into the retroviral expression vector pHNGAP, which contains a neomycin resistance gene and a 5′-FLAG-tag [Abe et al., 2004]. This retroviral vector was subjected to nucleotide sequencing to verify the identity of the DNA.

Retrovirus particles were produced and used for transfection as described previously [Abe et al., 2004]. Briefly, the retrovirus vector plasmid and a packaging plasmid (pCGCGP) were co-transfected into 293 cells grown in 6-well plates via the calcium phosphate coprecipitation method. The pseudotyped viruses were collected 48 h after transfection and stored at –80°C until further use.

These retroviral vectors were used to infect 32D cells in the presence of 10 μg/mL protamine (Mochida Pharmaceutical Co. Ltd, Tokyo, Japan). G418 (GIBCO) was added after 48 h to select stable transfectants and establish 32D cell lines expressing truncated RUNX1 (32D/RUNX1_TR). The expression of the Flag-tagged protein from transfected vectors was confirmed by Western blotting with the M2 antibody (Sigma).

*Flow Cytometry*

The 32D and 32D/RUNX1_TR cells were incubated with phycoerythrin-conjugated anti-mouse Gr1 (eBioscience, San Diego, CA, USA) or FITC-conjugated anti-mouse G-CSF receptor (G-CSFR; Becton Dickinson, San Jose, CA, USA) for 30 min on ice and then washed with phosphate-buffered saline. The flow cytometric analysis was performed using a BD FACSCanto II flow cytometer and FACSDiva software (Becton Dickinson).

*Cell Proliferation (XTT) Assay*

The cells were seeded into 96-well plates at a density of $10^4$/well in 100 μL IMDM supplemented with 10% horse serum (GIBCO), 0.01 ng/mL mIL-3, and various concentrations of G-CSF. The plates were incubated at 37°C for 72 h before addition of sodium 3′-[1-(phenylaminocarbonyl)-3,4-tetrazolium]-bis(4-methoxy-6-nitro)benzene sulfonic acid hydrate (XTT; Dojin Chemical, Kumamoto, Japan). After 2 h incubation, the absorption in each well at 450 nm was measured using a microplate reader.

## Results

*Patient*

The 59-year-old man was initially diagnosed with AML with eosinophilia (FAB classification M4Eo) (Fig. 1B) and admitted to Fujita Health University in Au-

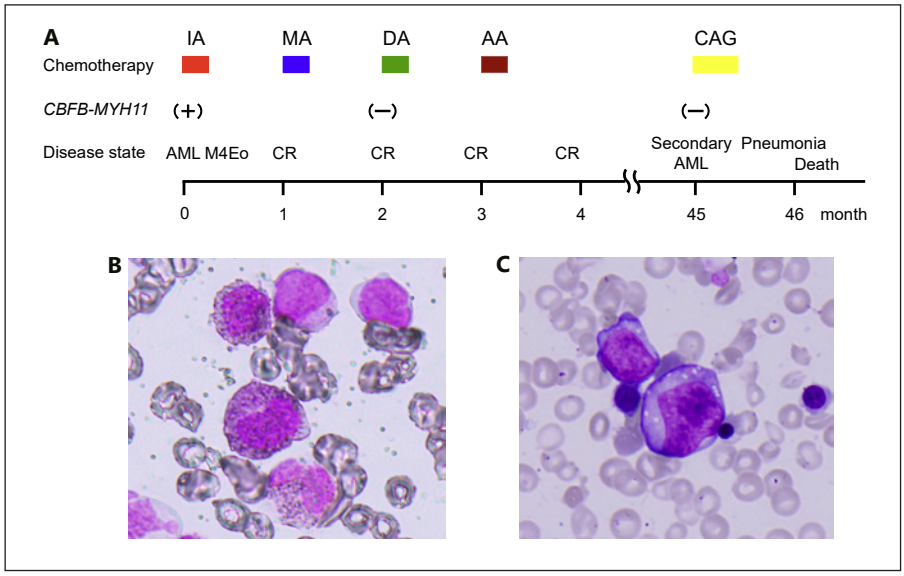


**Fig. 1.** Clinical course and morphological analysis of leukemia cells. **A** Chemotherapy regimen, *CBFB-MYH11*, and disease state are shown. IA, idarubicin + Ara-C; MA, mitoxantrone + Ara-C; DA, daunorubicin + Ara-C; AA, aclarubicin + Ara-C; CAG, Ara-C + aclarubicin + G-CSF; CR, complete remission. **B** At initial diagnosis, bone marrow aspirate smears revealed myelomonocytic blasts with eosinophils. **C** At secondary AML, bone marrow aspirate smears revealed monoblastic leukemia cells with vacuoles. **B**, **C** May-Grünwald-Giemsa staining, ×400.

gust 2008. His leukemia blasts exhibited the karyotype 46,XY,inv(16)(p13q22) and were positive for the core-binding factor subunit beta-myosin-heavy chain 11 (*CBFB-MYH11*) fusion gene. He was treated with a chemotherapy regimen of IA (idarubicin, cytarabine [Ara-C]), followed by 3 courses of consolidation therapy: MA (mitoxantrone, Ara-C), DA (daunorubicin, Ara-C), and AA (aclarubicin, Ara-C) (Fig. 1A). He achieved complete remission. However, he suffered a leukemia relapse 3 years later.

A bone marrow aspiration at the time of relapse revealed predominant monoblastic leukemia cells and an increased population of immature erythroid cells exhibiting dysplastic morphology (Fig. 1C). The relapsed leukemia blasts exhibited complex chromosomal aberrations without inv(16)(p13q22), and RT-PCR analysis did not detect the *CBFB-MYH11* fusion. A cytogenetic analysis of the bone marrow cells yielded the following karyotype: 44,XY,−3,der(5)t(5;17)(q11.2;q11.2)ins(5;?)(q11.2;?),−6,−14,−17,+mar1,+mar2[1]/43,idem,−7,−18,−21,+der(?)t(?;7)(?;q11.2),+mar3[4]/44,idem,der(7;14)(q10;q10),−21,+mar3,+mar4[2]. Upon analysis of single nucleotide variants (SNVs) from RNA-seq data, we found that the alteration of p53 G245S occurred at relapse with an allele frequency of 93.5% (online suppl. Table 2). Furthermore, we discovered that NOTCH1 Q1134R and other SNVs with high pathogenic scores were common in both initial and relapsed leukemia. Based on these findings, the patient was diagnosed with therapy-related AML. A single course of salvage therapy with CAG (Ara-C, aclarubicin, G-CSF) did not improve the patient's condition. He finally died of pneumonia and leukemia progression.

*Identification of* RUNX1-GRIK2as *Fusion Transcripts*

As described in Materials and Methods, we obtained and analyzed more than 51 million short paired-end reads from the patient's leukemia cDNA library. An RNA-seq analysis revealed a novel fusion of *RUNX1* at 21q22 with the antisense strand of the gene encoding glutamate receptor, ionotropic, kinase 2 (*GRIK2*) at 6q16 (*RUNX1-GRIK2as*; Fig. 2A). Fluorescence in situ hybridization (FISH) with a dual-color dual fusion translocation probe directed at the *RUNX1/RUNX1T1* chimera (Abbott Molecular/Vysis, Des Plaines, IL, USA) suggested the splitting of *RUNX1* signals (Fig. 2B). However, the cells were negative for the *RUNX1-RUNX1T1* fusion, and a spectral karyotyping analysis (SRL, Tokyo, Japan) did not reveal a rearrangement of 6q16 and 21q22 (online suppl. Fig. 1). In other words, the rearrangement between 6q16 and 21q22 was a cryptic abnormality.

*Multiple* RUNX1-GRIK2as *Transcripts and PCR Analysis*

We identified 5 fusion sites in *GRIK2*: 3 sites at intron 13 and 2 sites at intron 14 (Fig. 2A, 3A). Exon 6 of *RUNX1* was dominantly fused to the reverse sequence of *GRIK2*, whereas alternative splicing transcripts of *RUNX1* exon 5 were fused to *GRIK2* in each fusion transcript (Fig. 3A). A fusion to an antisense sequence may disrupt the normal splicing machinery via arbitrary splicing acceptors and

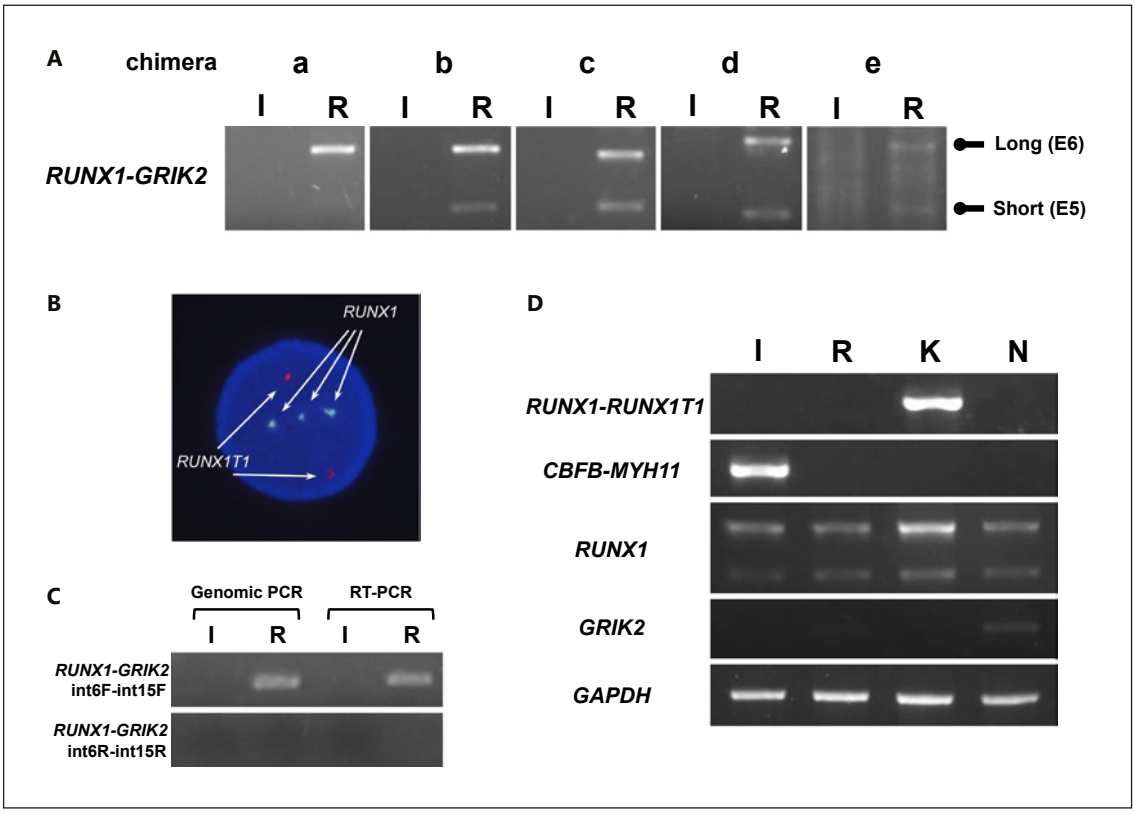


**Fig. 2.** PCR and FISH analyses. **A** RT-PCR analysis of *RUNX1-GRIK2* fusion genes. The fusion variants with splicing at the donor sites corresponding to the exon 5-intron 5 or exon 6-intron 6 junctions of *RUNX1* are defined as the short (E5) and long (E6) forms, respectively. **B** FISH analysis with a dual-color dual fusion translocation probe for the *RUNX1/RUNX1T1* chimeric gene yielded 3 *RUNX1* signals (blue), suggesting the splitting of this gene. The *RUNX1-RUNX1T1* fusion status was negative. **C** PCR analysis of the genomic breakpoint. The *RUNX1-GRIK2as* PCR product amplified from genomic DNA was the same size as that amplified from cDNA (primers: RUNX1_int6F, GRIK2_int15F). **D** Expression patterns of *CBFB-MYH11*, *RUNX1*, and *GRIK2*. *CBFB-MYH11* was determined at the initial diagnosis, but was negative at the time of relapse. Wild-type *RUNX1* and 2 splicing transcripts were detected at both time points and in the normal bone marrow, whereas *GRIK2* was detected in normal bone marrow and was absent or detectable at very low levels in leukemia cells. *GAPDH* was used as a positive control. I, initial diagnosis; R, relapse; K, the t(8; 21) Kasumi-1 cell line; N, normal bone marrow.

can yield multiple missplicing products. The alternative splicing transcripts used a standard splicing donor at the junctions of exon 5-intron 5 and exon 6-intron 6 of *RUNX1*, but unusual splicing acceptors in the antisense strand of *GRIK2* (Fig. 3B). The GT-AG splicing sites remained regulated in these transcripts. Approximately 58% of leukemia clones harbored *RUNX1-GRIK2as* according to an estimate from the number of reads mapped to the *RUNX1* ex6-ex7 or *RUNX1* ex6-*GRIK2* junction (Fig. 4A). The type d fusion transcript of *RUNX1* ex6-*GRIK2as* appeared to be the most frequent (Fig. 4A). Moreover, the very low number of reads mapped to the 5′-region of *GRIK2* suggested that the transcriptional activity of *GRIK2* was repressed (Fig. 4B).

Our RNA-seq analysis further identified a genomic breakpoint located in *RUNX1* intron 6 and *GRIK2* intron 15 (Fig. 3A). The RT-PCR amplification band between the 5′-ends of *RUNX1* intron 6 and *GRIK2* intron 15 was identical to that generated by the PCR amplification of genomic DNA using the same primers. The intronic sequences around the breakpoint were transcribed to RNA, and a reciprocal fusion of the 3′-end of *RUNX1* intron 6 to the 3′-end of *GRIK2* intron 15 was not detected (Fig. 2C). No expression of *GRIK2* was observed in the patient's relapsed leukemia cells (Fig. 2D), which expressed the normal allele of *RUNX1* (Fig. 2D) with no detectable mutation.

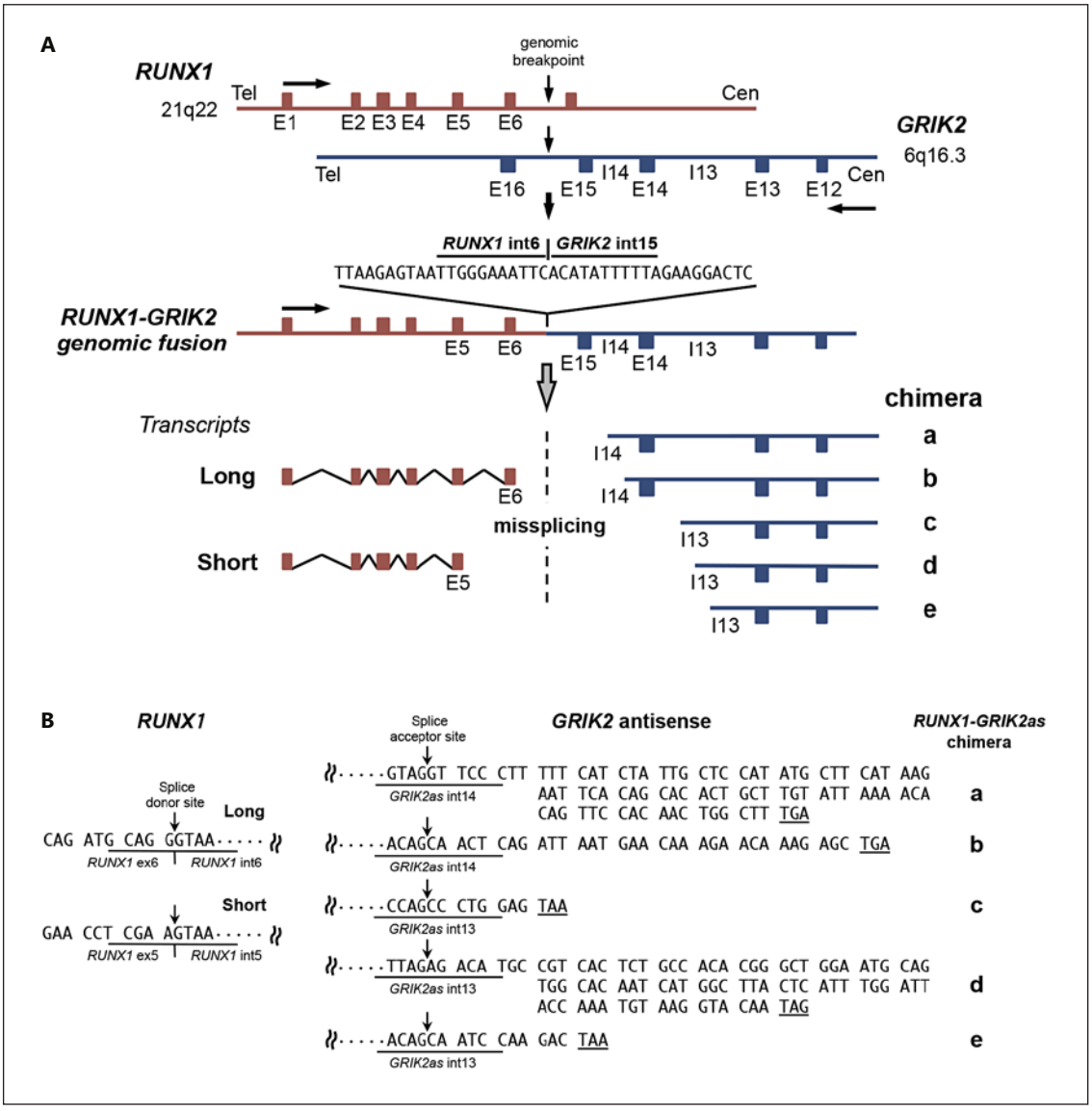


**Fig. 3.** Schematic structure and sequence of the *RUNX1-GRIK2as* fusion. **A** The fusion transcripts were transcribed by the *RUNX1* promoter and fused to the antisense strands of *GRIK2* (*RUNX1-GRIK2as*). *RUNX1* was spliced at the exon 5-intron 5 (short) or exon 6-intron 6 (long) junction to form the *RUNX1-GRIK2as* fusion. The antisense strand of *GRIK2* contained 5 splicing acceptor sites, and fusions with these different sites are designated as chimeras a–e. **B** DNA sequences around the fusion sites. The reading frame is distinguished by a space. Predicted stop codons are underlined. The common sequences of the splicing donor sites (GT) and acceptor sites (AG) were conserved. E, exon; I, intron; Tel, telomere; Cen, centromere.

*Enhanced Proliferation of 32D/RUNX1_TR Cells in Response to G-CSF*

The 32D cells transduced stably with the vector encoding *RUNX1-GRIK2as* expressed truncated *RUNX1* but could not be maintained without mIL-3. Moreover, these cells did not exhibit any proliferative advantage in response to mIL-3. We next analyzed the proliferative response of these 32D/RUNX1_TR cells to G-CSF, as the expression of G-CSFR on the surfaces of 32D cells is induced by mIL-3 depletion. As G-CSF was not sufficient for the maintenance of these cells, we examined the proliferative response to G-CSF in the presence of a low concentration of mIL-3 (0.01 ng/mL). Notably, the 32D/RUNX1_TR cells exhibited an enhanced proliferative re-

**A**

| | Reads mapped on *RUNX1* ex6–ex7 junction | Reads mapped on *RUNX1* ex6–*GRIK2* junction | | | | |
|---|---|---|---|---|---|---|
| Number of reads | 95 | 39 | | | | |
| Variants | – | a | b | c | d | e |
| Number of reads | – | 2 | 2 | 2 | 27 | 6 |

**B**

| | *GRIK2* | | | | | | | | | | | | | | | |
|---|---|---|---|---|---|---|---|---|---|---|---|---|---|---|---|---|
| Exon no. | 1 | 2 | 3 | 4 | 5 | 6 | 7 | 8 | 9 | 10 | 11 | 12 | 13 | 14 | 15 | 16 |
| Number of reads | 1 | 0 | 0 | 0 | 0 | 0 | 0 | 0 | 0 | 0 | 2 | 0 | 0 | 7 | 2 | 1 |
| Intron no. | 1 | 2 | 3 | 4 | 5 | 6 | 7 | 8 | 9 | 10 | 11 | 12 | 13 | 14 | 15 | – |
| Number of reads | 2 | 0 | 0 | 0 | 14 | 21 | 0 | 2 | 22 | 33 | 26 | 1 | >300 | 97 | 3 | – |

**Fig. 4.** Analysis of *RUNX1* and *GRIK2* mapping data. **A** The numbers of reads mapped to the *RUNX1* ex6-ex7 junction and *RUNX1* ex6-*GRIK2* junction. The reads mapped to the *RUNX1* ex6-*GRIK2* junction were subclassified to variants labeled chimeras a–e. Variant chimera d was dominant. The estimated percentage of leukemia clones harboring *RUNX1-GRIK2as* was approximately 58%. **B** The number of reads mapped to the *GRIK2* exon and intron. The 5′-region of *GRIK2* was not expressed. Therefore, the antisense strand of the 3′-region of *GRIK2* was transcribed from *RUNX1* in *RUNX1-GRIK2as*.

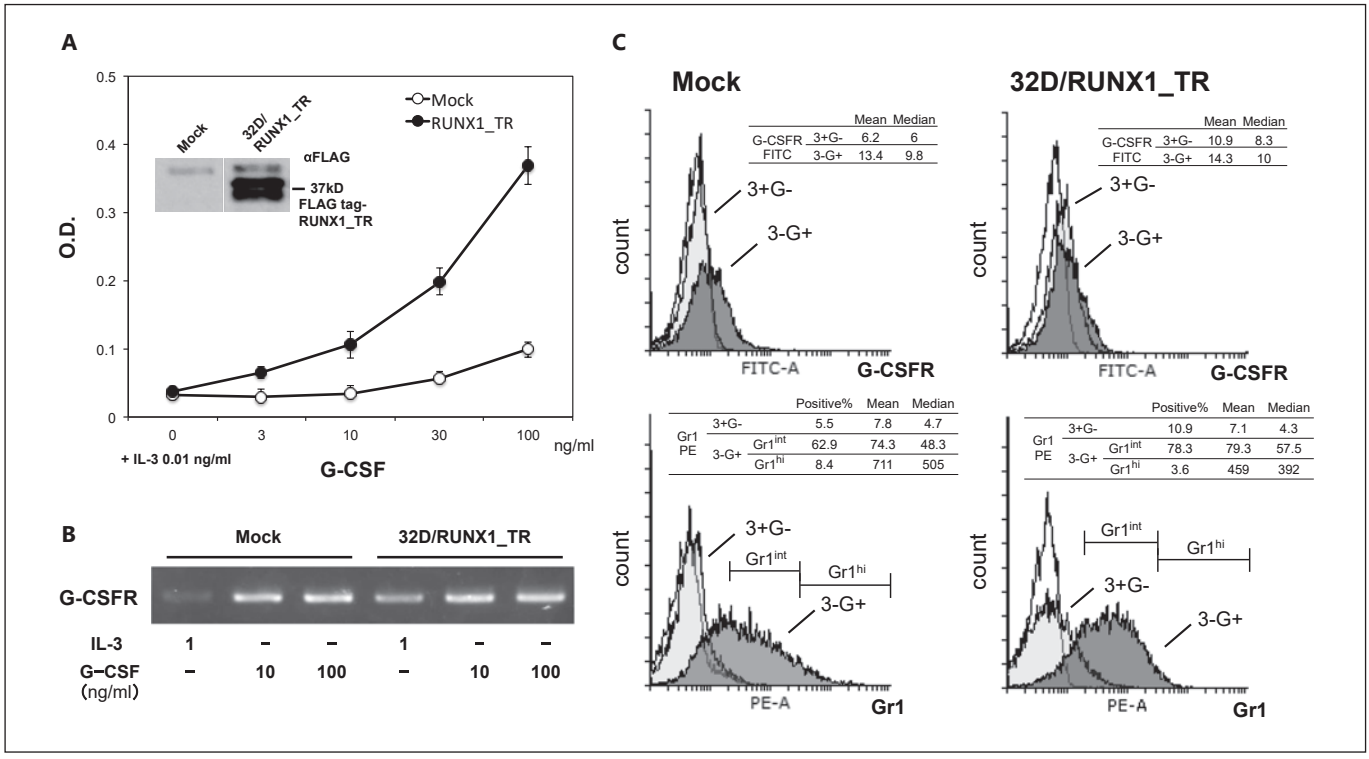


**Fig. 5.** Proliferation and differentiation of 32D/RUNX1_TR cells in response to G-CSF. **A** Proliferative responses of 32D/Mock and 32D/RUNX1_TR cells to G-CSF. The latter cells were infected with a lentiviral vector engineered to express truncated RUNX1. The cells ($10^4$ per well) were cultured for 3 days in the presence of 0.01 ng/mL mIL-3 and the indicated concentrations of G-CSF. Viable cells were measured using the XTT assay. A Western blot analysis demonstrates the presence of truncated RUNX1 protein (37 kDa) in 32D/RUNX1_TR cells. The data are shown from one representative of 3 replicated independent experiments. **B** RT-PCR analysis of the expression of the G-CSF receptor gene (*GCSFR*) in 32D/Mock and 32D/RUNX1_TR cells. The expression of *GCSFR* was induced after depleting mIL-3 and adding G-CSF. The expression of *GCSFR* in 32D/RUNX1_TR cells was higher than that in wild-type 32D cells cultured in the presence of mIL-3. **C** Flow cytometry analysis of the expression of G-CSFR and the myeloid differentiation antigen Gr1 in 32D/Mock and 32D/RUNX1_TR cells cultured in the presence of 100 ng/mL G-CSF for 5 days. Both cell types were cultured in IMDM supplemented with 10% FBS. G-CSFR was expressed on 32D/RUNX1_TR cells even in the presence of mIL-3. Representative data are shown.

**Table 1.** C-terminally truncated RUNX1 resulting from *RUNX1* translocation

| Original name of chimeric gene | HGNC symbol of partner gene | Location | Type of disease | Breakpoints of fusion transcripts | | Reference |
|---|---|---|---|---|---|---|
| | | | | *RUNX1* | partner gene: fusion type | |
| *RUNX1-EAP* | *RPL22* | 3q26 | tAML, tMDS, CML BC | exon 5<br>exon 6 | *RPL22*: exon 2, out of frame | Nucifora et al., 1994 |
| *RUNX1-AMP19* | ND | 19q13.4 | Radiation-associated AML | exon 5<br>exon 6 | IGR[a]<br>to *NLRP4*: intron 8, antisense | Hromas et al., 2001 |
| *RUNX1-Copine VIII* | *CPNE8* | 12q12 | AML | exon 6 | IGR[b] | Ramsey et al., 2003 |
| *RUNX1-DTX2* | *DTX2* | 7q11.2 | AML | exon 6 | *UPK3B*: exon 2, antisense;<br>*UPK3B*: intron 1, antisense<br>to *DTX2*: exon 10, antisense | Maki et al., 2012 |
| *RUNX1-SV2B* | *SV2B* | 15q26.1 | AML | exon 1 | *SV2B*: intron 1, antisense | Giguère and Hébert, 2013 |
| *RUNX1-TMEM48* | *NDC1* | 1p32 | MDS/AML | intron 5 | *NDC1*: intron 3, antisense | Rodriguez-Perales et al., 2016 |
| ND | ND | 6q25 | AML | exon 6 | IGR | Panagopoulos et al., 2016 |
| *RUNX1-PRPF38A* | *PRPF38A* | 1p32 | AML | exon 6 | *PRPF38A*: exon 1, out of frame | Wang et al., 2017 |
| *RUNX1-GRIK2* | *GRIK2* | 6q16.3 | AML relapse | exon 5<br>exon 6 | *GRIK2*: intron 13, antisense<br>intron 14, antisense | Present case |

CML BC, chronic myeloid leukemia blast crisis; HGNC, HUGO Gene Nomenclature Committee; IGR, intergenic region; ND, not determined; tAML, therapy-related acute myeloid leukemia; tMDS, therapy-related myelodysplasia. [a] Between *NLRP4* and *NLRP13*. [b] 73 kb upstream of *CPNE8*.

sponse to G-CSF (Fig. 5A). Interestingly, RUNX1_TR induced the expression of G-CSFR even in the presence of mIL-3 (Fig. 5B, C).

Gr1 is a cell surface antigen expressed during the maturation of myeloid cells. G-CSF induces the granulocytic differentiation of 32D cells by upregulating the expression of Gr1 [Schuster et al., 2003]. Accordingly, we assessed the frequencies of $Gr1^{int}$ and $Gr1^{hi}$ cells to determine the effect of G-CSF on the myeloid differentiation of 32D cells. Although RUNX1_TR did not impair the expression of Gr1 on 32D cells in the presence of G-CSF, a mild increase in the $Gr1^{int}$ fraction and modest decrease in the $Gr1^{hi}$ fraction were observed in 32D/RUNX1_TR cells relative to 32D cells (Fig. 5C).

## Discussion

In this case, our patient was initially diagnosed with AML harboring the *CBFB-MYH11* fusion. Upon relapse, however, his leukemia cells were negative for *CBFB-MYH11* and exhibited complex chromosomal abnormalities. An RNA-seq analysis revealed the occasional fusion of *RUNX1* at 21q22 to *GRIK2* at 6q16 via a cryptic rearrangement that was not identified by G-band and spectral karyotyping analyses.

*TP53* mutations have an increased incidence rate in therapy-related AML [Wong et al., 2015]. Initial leukemia cells were diagnosed as AML M4Eo with several pathogenic SNVs in addition to *CBFB-MYH11*, in particular NOTCH1 Q1134R, which is known as a recurrent alteration in Chinese oral squamous cell carcinoma [Song et al., 2014]. Although *CBFB-MYH11* was not detected in the relapsed leukemia cells, based on the preleukemic clones harboring pathogenic SNVs, we believe that the *TP53* mutation caused therapy-related AML.

Glutamate receptors mediate the majority of excitatory neurotransmissions in the brain. *GRIK2* produces a protein with a distinct role in glutamatergic neurotransmission and neuronal development as well as a potential tumor-suppressing capacity [Sinclair et al., 2004]. Notably, *TRMT11-GRIK2* fusion genes have been reported in 7.9% of prostate cancer cases, where the loss of function is predicted to contribute to tumorigenesis [Yu et al., 2014]. In our case of AML, very low levels of expression of the 5′-end of *GRIK2* were detected in the patient's leukemia cells via RNA-seq and RT-PCR analyses. Therefore, the pathogenesis of the *RUNX1-GRIK2* fusion may depend on the aberrantly truncated RUNX1 product produced by *RUNX1-GRIK2as*.

To date, 9 types of translocations predicted to produce aberrantly truncated forms of RUNX1 have been reported (Table 1). *RUNX1-EAP* is an out-of-frame fusion [Nucifora et al., 1994], while *RUNX1-AMP19* and *RUNX1-Copine VIII* [Hromas et al., 2001; Ramsey et al., 2003] are fusions of *RUNX1* to noncoding intergenic regions. Panagopoulos et al. [2016] reported a similar RUNX1 truncation resulting from a fusion to an intergenic sequence

on 6q25. *RUNX1-DTX2*, *RUNX1-SV2B*, and *RUNX1-TMEM48* are fusions with the antisense strands of the respective partner genes. These fusions disrupt the normal splicing machinery and yield fusion transcripts that include intron regions [Maki et al., 2012; Giguère and Hébert, 2013; Rodriguez-Perales et al., 2016]. *RUNX1-PRPF38A* is a fusion of *RUNX1* to the 5′ noncoding sequence in exon 1 of *PRPF38A* [Wang et al., 2017]. Most fusion sites of *RUNX1* involve exon 6, although *RUNX1-SV2B* and *RUNX1-TMEM48* involve exon 1 and intron 5, respectively. *RUNX1-DTX2* produces an aberrant C-terminally truncated RUNX1 via the fusion of *RUNX1* to *UPK3B-DTX2* reverse sequences. This truncated protein is reported to act as a dominant negative inhibitor of RUNX1 [Maki et al., 2012].

The exogenous expression of truncated RUNX1 from *RUNX1-TMEM48* increases the proliferation and self-renewal of human hematopoietic/progenitor stem cells [Rodriguez-Perales et al., 2016]. Chin et al. [2016] reported that in mouse bone marrow, *Runx1* haploinsufficiency promotes the hypersensitivity of hematopoietic stem and progenitor cells to G-CSF and impedes G-CSF-induced granulopoiesis, leading to the accumulation of $Gr1^{int}$ granulocytes. Here, we demonstrate that in 32D cells, truncated RUNX1 enhanced proliferation in response to G-CSF and induced G-CSFR expression. In these cells, RUNX1_TR expression led to a mild increase of the $Gr1^{int}$ fraction in the presence of G-CSF.

Taken together, we have identified *GRIK2* as a novel fusion partner for *RUNX1*, and demonstrated that this fusion is chimerized in the reverse direction via a cryptic chromosome translocation between 6q16 and 21q22. This *RUNX1-GRIK2as* fusion supports the importance of aberrantly truncated RUNX1 in leukemogenesis.


## Acknowledgements

We greatly appreciate the technical assistance of Dr. Hidehito Inagaki and Dr. Hiroki Kurahashi (Genome and Transcriptome Analysis Center, FHU) during next-generation sequencing. We also thank Sachiko Iba and Keiko Hattori for their valuable laboratory assistance. The authors would like to thank Enago (www.enago.jp) for the English language review.


## Statement of Ethics

The patient provided written informed consent for the isolation of mononuclear cells from his bone marrow. This study has been approved by Human Genome, Gene Analysis Research Ethics Committee of Fujita Health University.

## Disclosure Statement

The authors have no conflicts of interest relevant to this report to declare.


## Funding Sources

This work was supported by JSPS KAKENHI Grant Number 16K09860 to A.A., a Grant-in-Aid from Fujita Health University to N.E., and the Program for the Strategic Research Foundation at Private Universities supported by the Ministry of Education, Culture, Sports, Science, and Technology (MEXT).


## Author Contributions

A.A. and Y.Y. performed the research and the gene analysis, and drafted the manuscript. N.E. and A.T. designed the research. A.K. revised the manuscript and added various comments as well as the interpretation of the results. H.Y., A.O., Y.I., C.I., M.T., and M.O. assessed the clinical data of the patient. All authors read and approved the final manuscript.

## References


Abe A, Emi N, Kanie T, Imagama S, Kuno Y, et al: Expression cloning of oligomerization-activated genes with cell-proliferating potency by pseudotype retrovirus vector. Biochem Biophys Res Commun 320:920–926 (2004).

Cancer Genome Atlas Research Network: Genomic and epigenomic landscapes of adult de novo acute myeloid leukemia. N Engl J Med 368:2059–2074 (2013).

Chin DW, Sakurai M, Nah GS, Du L, Jacob B, et al: *RUNX1* haploinsufficiency results in granulocyte colony-stimulating factor hypersensitivity. Blood Cancer J 6:e379 (2016).

De Braekeleer E, Ferec C, De Braekeleer M: *RUNX1* translocations in malignant hemopathies. Anticancer Res 29:1031–1037 (2009).

Giguère A, Hébert J: Identification of a novel fusion gene involving *RUNX1* and the antisense strand of *SV2B* in a *BCR-ABL1*-positive acute leukemia. Genes Chromosomes Cancer 52: 1114–1122 (2013).

Hromas R, Busse T, Carroll A, Mack D, Shopnick R, et al: Fusion AML1 transcript in a radiation-associated leukemia results in a truncated inhibitory AML1 protein. Blood 97:2168–2170 (2001).

Ichikawa M, Yoshimi A, Nakagawa M, Nishimoto N, Watanabe-Okochi N, Kurokawa M: A role for RUNX1 in hematopoiesis and myeloid leukemia. Int J Hematol 97:726–734 (2013).

Kim D, Salzberg SL: TopHat-Fusion: an algorithm for discovery of novel fusion transcripts. Genome Biol 12:R72 (2011).

Maki K, Sasaki K, Sugita F, Nakamura Y, Mitani K: Acute myeloid leukemia with t(7;21)(q11.2;q22) expresses a novel, reversed-sequence *RUNX1-DTX2* chimera. Int J Hematol 96:268–273 (2012).

McPherson A, Hormozdiari F, Zayed A, Giuliany R, Ha G, et al: deFuse: an algorithm for gene fusion discovery in tumor RNA-Seq data. PLoS Comput Biol 7:e1001138 (2011).

Miyoshi H, Kozu T, Shimizu K, Enomoto K, Maseki N, et al: The t(8;21) translocation in acute myeloid leukemia results in production of an *AML1-MTG8* fusion transcript. EMBO J 12:2715–2721 (1993).

Nucifora G, Begy CR, Kobayashi H, Roulston D, Claxton D, et al: Consistent intergenic splicing and production of multiple transcripts between *AML1* at 21q22 and unrelated genes at 3q26 in (3;21)(q26;q22) translocations. Proc Natl Acad Sci USA 91:4004–4008 (1994).

Owen C, Barnett M, Fitzgibbon J: Familial myelodysplasia and acute myeloid leukaemia – a review. Br J Haematol 140:123–132 (2008).

Panagopoulos I, Torkildsen S, Gorunova L, Ulvmoen A, Tierens A, et al: *RUNX1* truncation resulting from a cryptic and novel t(6;21)(q25;q22) chromosome translocation in acute myeloid leukemia: a case report. Oncol Rep 36:2481–2488 (2016).

Ramsey H, Zhang DE, Richkind K, Burcoglu-O'Ral A, Hromas R: Fusion of AML1/Runx1 to copine VIII, a novel member of the copine family, in an aggressive acute myelogenous leukemia with t(12;21) translocation. Leukemia 17:1665–1666 (2003).

Rodriguez-Perales S, Torres-Ruiz R, Suela J, Acquadro F, Martin MC, et al: Truncated RUNX1 protein generated by a novel t(1;21)(p32;q22) chromosomal translocation impairs the proliferation and differentiation of human hematopoietic progenitors. Oncogene 35:125–134 (2016).

Schuster C, Forster K, Dierks H, Elsasser A, Behre G, et al: The effects of Bcr-Abl on C/EBP transcription-factor regulation and neutrophilic differentiation are reversed by the Abl kinase inhibitor imatinib mesylate. Blood 101:655–663 (2003).

Sinclair PB, Sorour A, Martineau M, Harrison CJ, Mitchell WA, et al: A fluorescence in situ hybridization map of 6q deletions in acute lymphocytic leukemia: identification and analysis of a candidate tumor suppressor gene. Cancer Res 64:4089–4098 (2004).

Song X, Xia R, Li J, Long Z, Ren H, et al: Common and complex *Notch1* mutations in Chinese oral squamous cell carcinoma. Clin Cancer Res 20:701–710 (2014).

Tsuzuki S, Hong D, Gupta R, Matsuo K, Seto M, Enver T: Isoform-specific potentiation of stem and progenitor cell engraftment by *AML1/RUNX1*. PLoS Med 4:e172 (2007).

Wang H, Chen X, Xu Z, Tan Y, Qi X, et al: Identification of a novel fusion gene, *RUNX1-PRPF38A*, in acute myeloid leukemia. Int J Lab Hematol 39:e90–e93 (2017).

Wong TN, Ramsingh G, Young AL, Miller CA, Touma W, et al: Role of *TP53* mutations in the origin and evolution of therapy-related acute myeloid leukaemia. Nature 518:552–555 (2015).

Yu YP, Ding Y, Chen Z, Liu S, Michalopoulos A, et al: Novel fusion transcripts associate with progressive prostate cancer. Am J Pathol 184:2840–2849 (2014).